Validation of the Functions and Prognostic Values of Synapse Associated Proteins in Lower-Grade Glioma

Han Lin
Guangdong Academy of Medical Sciences: Guangdong Provincial People's Hospital
Yong Yang
Guangdong Academy of Medical Sciences: Guangdong Provincial People's Hospital
Chongxian Hou
Guangdong Academy of Medical Sciences: Guangdong Provincial People's Hospital
Jiantao Zheng
Guangdong Academy of Medical Sciences: Guangdong Provincial People's Hospital
Guangzhao Lv
Guangdong Academy of Medical Sciences: Guangdong Provincial People's Hospital
Rui Mao
Guangdong Academy of Medical Sciences: Guangdong Provincial People's Hospital
Peihong Xu
Guangdong Academy of Medical Sciences: Guangdong Provincial People's Hospital
Shanwei Chen
Guangdong Academy of Medical Sciences: Guangdong Provincial People's Hospital
Yujun Zhou
Guangdong Academy of Medical Sciences: Guangdong Provincial People's Hospital
Peng Wang
Guangdong Academy of Medical Sciences: Guangdong Provincial People's Hospital
Dong Zhou (zhoudong5413@163.com)
Guangdong General Hospital https://orcid.org/0000-0002-3289-2168

Primary research

Keywords: Synapse, synapse associated protein, lower-grade glioma, prognosis, seizure

Posted Date: September 26th, 2020

DOI: https://doi.org/10.21203/rs.3.rs-80139/v2

Version of Record: A version of this preprint was published at Bioscience Reports on May 1st, 2021. See the published version at https://doi.org/10.1042/BSR20210391.

Abstract

Background: Synapse and synapse associated proteins (SAPs) play critical roles in various neurodegeneration diseases and brain tumors. However, in lower-grade gliomas (LGG), SAPs have not been explored systematically. Herein, we are going to explore SAPs expression profile and its clinicopathological significance in LGG which can offer new insights to glioma therapy.

Method: In this study, we used five sources including, Venkatesh, Shen, Colón, Jüttner R, Gene Ontology (GO) project to integrate a list of SAPs that covered 231 proteins with synaptogenesis activity and post synapse formation. The LGG RNA-seq data were downloaded from gene expression omnibus (GEO) database, The Cancer Genome Atlas (TCGA), and Chinese Glioma Genome Atlas (CGGA). The differentially expressed SAPs were filtered out and constructed PPI to search for key modules and SAPs. Then, using Kaplan–Meier survival analysis, least absolute shrinkage and selection operator (LASSO), and multicox regression analysis, the prognostic significance of these key SAPs was evaluated. CGGA database, Human Protein Altas (HPA) and quantitative real-time PCR were used to verify our findings.

Result: Data from function enrichment analysis revealed functions of differentially expressed SAPs in synapse organization and glutamatergic receptor pathway in LGGs. Survival analysis revealed four SAPs, GRIK2, GABRD, GRID2, ARC that were correlate with the prognosis of LGG patients and used to construct the prognostic models. Among them, the expression of GABRD was lower in glioma tissue than normal brain tissue, but higher in seizure LGG patients than non-seizure patients. The four-SAPs signature was revealed as an independent prognostic factor in gliomas.

Conclusion: Our study presented a novel strategy to assess the prognostic risks of LGGs, based on the expression of SAPs. Also, we revealed that several SAPs upregulated in patients with seizures, indicating that they are linked to the pathogenesis of seizures in glioma patients.

Introduction

Glioma is the most prevalent neuroepithelial malignant tumor associated with poor prognosis, high disability, and high recurrence rates. Depending on the degree of malignancy, gliomas are classified into 4 grades (WHO grades I, II, III, and IV). Among these, diffuse low-grade glioma and intermediated-grade glioma make up lower-grade gliomas (LGG, grade II and grade III glioma) (1). The variability in the prognosis and survival of LGG is attributed to the heterogeneity of its clinical behavior (2). LGG patients usually manifest as seizures, but in the course of the disease, glioma can also cause neurological and neurocognitive disorders or premature death. The impact of LGG surgical resection depends on the molecular subtype of the tumor and increases with the degree of tumor malignancy (3). Therefore, more investigations on the LGG and their biomarkers are essential for advanced therapy.

Synapse is specialized cytosolic structure in the nervous system. It is classified as chemical synapse and electrical synapse. Electrical synapse comprises gap junctions, forming the channel to transport ion, and producing electrical flux (4). On the other hand, the chemical synapse consists of pre-synapse, synaptic

cleft, post-synapse, which constructs the complex connection between neuron-neuron and neuron-glia, brick the intricacies and the sophistication of neuronal network configuration (5). Synapse associated protein (SAP) is the protein associated with synapse structure and formation, including neurotransmitter receptor, vesicle-associated protein, synaptogenesis factors, among others. Mutations or dysregulation of SAPs in the central nervous system causes synapse dysfunction, thereby promoting the progression of various neurodegenerative diseases (6-11). Recent studies reported that SAPs were significantly associated with malignancies in the brain (Fig.1). Also, breast metastases express neuroligin-2 and PSD-95 to form pseudo-tripartite synapses with neurons, which permits metastases to utilize glutamate and promote invasion in the brain (12). A study by Varun Venkataramani *et al.* demonstrated that synapses-like structure is formed between presynaptic neurons and postsynaptic glioma cells. Neuronal-to-glioma synapse (NGS) induced excitatory postsynaptic currents through AMAPR, which significantly contributes to the invasion and growth of glioma (13). In high-grade glioma (glioblastoma and grade III astrocytoma), the excitatory signal from NGS depolarizes glioma cells and amplify the signals via gap junction, thus promoting their proliferation. Furthermore, targeting neuroligin-3 (important synaptogenesis factors) effectively minimizes the growth of glioma (14, 15). Whilst acknowledging the roles of SAPs in the occurrence and development of high-grade glioma and breast metastasis, their functions in lower-grade glioma development are subtle. Therefore, additional and systematic research on SAPs will comprehensively impart knowledge about their functions in LGGs.

In this work, LGG RNA-seq and corresponding clinicopathological data were downloaded from gene expression omnibus (GEO) database, the cancer genome atlas (TCGA) database, and Chinese glioma genome atlas (CGGA). Then, differentially expressed SAPs between LGG samples and normal brain tissue were screened, and their potential bio-function explored. Our findings demonstrated that LGG-related SAPs might advance understanding of the glioma progression and manifestation hence providing insights into developing biomarkers for effective diagnosis and prognosis.

Materials And Methods

Screening of SAPs and data processing

A list of human synapse associated proteins from five sources were integrated including, Venkatesh, Shen, Colón, Jüttner R, Gene Ontology (GO) project (Supplement Table 1) (14, 16-18). The RNA-seq data for Rembrandt were downloaded from GEO (GSE68848), which contained 183 LGG samples and 28 normal brain tissue samples. Besides, the RNA-sequencing data from Henry Ford Hospital were downloaded from GEO (GSE4290) and contained 76 LGG samples and 23 normal brain tissue samples. Using the Limma R-package, differentially expressed genes between normal brain tissue and LGG were identified. In total, 523 and 576 LGG samples with corresponding clinical data were downloaded from The Cancer Genome Atlas database (TCGA, https://portal.gdc.cancer.gov/) and Chinese Glioma Genome Atlas (CGGA, http://www.cgga.org.cn/) respectively.

Functional enrichment analysis of differentially expressed SAPs

Through DAVID (https://david.ncifcrf.gov/), GO component and Kyoto encyclopedia of genes and genomes (KEGG) analyses were performed on differentially expressed SAPs to determine their bio-functions (P<0.05 and FDR<0.05). WEB-based Gene Set Analysis Toolkit (http://www.webgestalt.org/) was used to validate the functional enrichment result.

Protein-protein interaction network construction

Using the STRING database (https://string-db.org/), the protein-protein interaction (PPI) between all differentially expressed SAPs was assessed, and their network was constructed using Cytoscape 3.7.1. Then, the MCODE (Molecular Complex Detection) function was applied to screen key modules SAPs from the network (score> 7 and node number > 5).

Prognosis-related SAPs selection

The univariate Cox regression model was used to determine the prognostic significance of key SAP was with. Subsequently, the least absolute shrinkage and selection operator (LASSO) was exploited to identify the prognostic significance of candidate SAPs (iteration =1000). SAP with a P-value of less than 0.05 was considered to be candidate prognostic SAPs.

Predictive model construction

Based on the candidate prognostic SAPs genes, we developed a multivariate Cox proportional hazards regression model to predict the prognosis of LGG patients. The risk score of each sample was calculated using the formula:

$$\text{Risk score} = \sum_{i=1}^{n} \beta_i \text{Exp}_i$$ (β=coefficient value; Exp=gene expression level)

LGG patients in the TCGA cohort were subdivided into high-risk groups and low-risk groups according to the median risk score. A log-rank test was performed to compare the OS difference between low-risk and high-risk groups. ROC (Receiver Operating Characteristic) curve was plotted to estimate the performance of the predictive model. Next, patient samples from the CGGA cohort were used as the validation set to verify the predictive capability of our model. Finally, the nomogram (a statistical model) and calibration plots were implemented to foresee the possibility of OS. P<0.05 was considered statistically significant.

Mutation and copy number alteration of SAPs

Based on 2200 LGGs from TCGA, MSK, MSLCC and UCSF, mutation and copy-number alteration data for all hub SAPs were identified via the GISTIC algorithm and segmentation analysis in cBioPortal6 (http://www.cbioportal.org/) (19, 20).

Expression and prognostic value verification

A Violet plot was established to display the mRNA expression difference between LGG and normal brain tissue in the Rembrandt cohort and Henry Ford Hospital cohort. Using the Human Protein Atlas (HPA) online database (http://www.proteinatlas.org/), the expression of hub SAPs at a translational level was detected. The survival R-package was used to evaluate the prognostic value of the hub SAPs in LGGs with the Kaplan-Meier technique. Also, the association between the expression of hub SAPs and clinicopathologic features was evaluated.

Quantitative Real-time PCR

A total of 15 samples, including 10 samples from patients with LGG and 5 from normal brain tissue, were used for Quantitative real-time PCR verification of the expression of key genes. In brief, total RNAs were isolated using a TRIzol reagent (Invitrogen). Later, using the PrimeScript RT Master Mix (Takara, China), we synthesized the cDNA and performed PCR with the SYBR GREEN kit (Takara, China) in the BIO RAD Real-Time PCR System. The primers used in this study are listed in Table 1.

Statistical analysis

Statistical analysis was performed with GraphPad Prism software version 8.0 using the mann-whitney-u test. According to the median value of SAPs, the samples in the data were divided into a low expression group and a high expression group. OS is presented as the Kaplan-Meier curve. $P<0.05$ was regarded as statistically significant.

Results

Identification of differentially expressed SAPs in LGG Patients

The study design is illustrated in Figure 2. The R software was adopted to identify the differentially expressed SAPs from a sum of 201 SAPs. A total of 112 SAPs was screened out ($P<0.05$, $|\log2FC| > 0.5$), which carried 44 downregulated and 68 upregulated SAPs (Fig.3, Table 2).

Functional enrichment analysis of the differently expressed SAPs

To scrutinize the bio-function of identified SAPs, the SAP genes were grouped in accordance with their expression level. Subsequently, the online tool DAVID and WebGestalt was used to conduct a functional enrichment analysis of these groups. The upregulated differentially expressed SAPs were enriched in biological processes (BP) related to the regulation of trans-synaptic signal, and synapse organization and post synapse organization (Fig.4A and 4E). While the downregulated differentially expressed SAPs were significantly enriched in modulation of chemical synaptic transmission, synapse organization, and dendritic spine organization (Fig.4B and 4F). The molecular function (MF) analysis revealed that the upregulated SAPs were markedly enriched in ionotropic glutamate receptor activity, neurexin family protein binding, and glutamate receptor activity (Fig.4A and 4E), whereas the downregulated SAPs were

significantly enriched in ion gated channel activity, gated channel activity, and substrate-specific channel activity (Fig.4B and 4F). In terms of the cellular component (CC), the downregulated SAPs were primarily enriched in the presynapse, cell junction, and ion channel complex, and upregulated SAPs were significantly enriched in the postsynaptic membrane and glutamate synapse (Fig.4B and 4F). Besides, we found that upregulated SAPs were enriched in cell adhesion molecules pathway, glutamatergic synapse, and neuroactive ligand-receptor interaction pathway (Fig.4C and 4G). Furthermore, downregulated differentially expressed SAPs were mainly enriched in the calcium signaling and Nicotine addiction (Fig.4D and 4H).

Construction of PPI network and key modules

Based on the STRING database and Cytoscape software, the PPI network was constructed, which included 94 nodes and 563 edges. Subsequently, the PPI network was analyzed to screen for potential key modules using MODE in Cystoscope. Module 1 contained 23 nodes and 102 edges, module 2 included 12 nodes and 48 edges, module 3 consisted of 5 nodes and 10 edges. Then, the KEGG pathway and GO analyses demonstrated that the SAPs in module 1 were enriched in the glutamatergic synapse, glutamate receptor signaling pathway, synaptic membrane, neurexin family protein binding. The SAPs genes in module 2 were enriched in neuroactive ligand-receptor interaction, regulation of ion transmembrane transporter activity, synaptic membrane, and glutamate receptor activity. The SAPs in module 3 were enriched in GABAergic synapse, chloride transmembrane transport, chloride channel complex, and chloride channel activity (Fig. 5).

Selection of a prognostic-related SAPs

To analyze the prognostic significance of the key SAPs in key modules, univariate Cox regression analysis was used and obtained 20 prognostic-associated SAPs (Fig.6A). These candidate SAPs were analyzed by lasso regression analysis and multiple stepwise Cox regression analysis and four hub SAPs were identified as the independent predictors in LGG patients (Fig.6B-6D).

Copy-number alteration and mutation analysis of SAPs in LGG patients

Copy-number alteration (CNA) analyses and mutation of SAPs were conducted using the GISTIC algorithm and segmentation analysis in cBioPortal6. The results showed that hub SAP genes were altered in 82 samples out of 2200 LGG patients (4%) (Fig. 7E).

Validation of Expression and Prognostic Value of hub SAPs in LGGs

Compared with that in normal brain tissue, the expression of GRIK2, GRID2 and ARC were higher and GABRD was lower in LGGs (Fig. 7A and 7B). The result of quantitative real-time PCR confirmed the outcome mentioned above (Fig. 7C). From the Human Protein Atlas database, immunohistochemistry results showed that GIRD2 and GRIK2 were upregulated in gliomas than normal brain tissue. On the contrary, GABRD were downregulated in glioma tissue (Fig. 7D). Furthermore, we used the Kaplan Meier-plotter method to probe the relationship between OS and hub SAPs. Results indicated that the expression

of hub SAPs was associated with the prognosis of LGG patients (Fig. 8A-8D). The CGGA cohort was used to validate the prognostic value of hub SAPs (Supplementary Fig. 1). The expression of hub SAPs seems to correlate with LGG grades and patients' age (Fig.8E-8L). Besides, GABRD was upregulated in seizure LGG patients (Fig.8N).

Construction and analysis of a prognostic score model

The prognostic score model was constructed following the hub SAPs. The risk score of each patient was calculated according to the following formula:

Risk score= (-0.19806*ExpGRID2) + (0.248830*ExpARC) + (-0.267494*ExpGRIK2) + (-0.503747*ExpGABRD)

Based on the median risk score, 524 LGG patients in the TCGA cohort were divided into high-risk and low-risk subgroups. Compared with patients in the low-risk subgroup, those in the high-risk subgroup exhibited a poorer OS (Fig. 9A). Then, a time-dependent ROC analysis was performed, which suggested that it has a good diagnostic performance (Fig. 9B). Besides, scatter plots were created to display the survival status of patients and the risk score of the signature in the high- and low-risk subgroups (Fig. 9D). Additionally, the prognostic value of the four-SAPs signature predictive model was assessed, and a similar formula was used to the CGGA cohort. Results revealed that LGG patients with high-risk scores have a significantly lower OS than those with low-risk scores in the CGGA cohort (Fig. 10A-10D).

Construction of nomogram based on the hub SAPs

Multivariate Cox regression analyses were used to estimate the prognostic significance of different clinical characteristics of glioma patients. Results indicated that the risk score was an independent prognostic factor associated with OS in glioma patients ($P<0.05$, Fig. 11A). Due to the clinical relevance and prognostic value of other clinicopathologic factors, we constructed a nomogram and applied it in evaluating survival rates for glioma patients at 1, 3, and 5 years, which could aid clinicians in setting clinical plans for glioma patients (Fig. 11B). The calibration plots presented good conformity between the predicted and observed outcomes in both the TCGA and CGGA cohorts (Fig. 11C and 11D).

Discussion

Non-specific treatments for glioma include surgical resection, radiotherapy, and chemotherapy, show a significant survival benefit in glioma patients. However, there is still no targeted therapy effective against glioma. The abundance of neurotransmitters in the central nervous system creates a special microenvironment for brain tumors where cancer cells can transduce neurotransmitter-mediated intracellular signaling pathways inducing their growth, activation, and metastasis (21). Since neurotransmitters are important for tumor growth, the speculation that tumor cells might stimulate their innervation with neuron was proven by the discovery of neuro-glioma synapses and metastasis-neuron synapses (22). These findings reveal a biologically crucial direct synaptic communication between

neurons and tumor cells with potential clinical implications. However, as far as we know, the prognostic value of synapse associated proteins in lower-grade glioma remains largely understudied.

In the current study, we performed functional enrichment analysis on differentially expressed SAPs. Biological processes or pathways that upregulate the expressed SAPs are majorly enriched in synapse organization and special neurotransmitter receptor signals which include glutamate receptor signals. In the peripheral neural system, synapse modulation and neurotransmitter signals influence the progression of many tumors, including pancreatic cancer and prostate cancer (23, 24). In endometrial cancer (EC), GluR2 (GRIA2) expression was upregulated, and the GluR2 antagonist effectively suppressed the invasion, migration, and proliferation of tumor cells. Both *in vitro* and *in vivo*, EC cells showed its tropism toward DRG neurons and neuron fiber which implied that glutamate receptor signal and neuron-tumor interaction play a significant role in EC growth (25). Moreover, in the central nervous system, previous studies demonstrated that the generation of synapse and glutamate receptor signals were linked to the progression of high-grade glioma and breast tumor patients, which corroborates with our results of LGG patients (12, 26-28).

To further explore the association between SAPs in LGGs, a protein-protein interaction network of these differently expressed SAPs was created where three key modules including 40 key SAPs were screened. Among them, many SAPs have been reported to participate in the development and progression of tumors. NLGN1, NLGN2, NLGN3, and NLGN4X are neuroligin family members that interact with presynaptic neurexins to regulate heterophilic adhesion. In the deep brain region, a high expression of NLGN3 was associated with glioblastoma recurrence (29). While in neuroblastoma, NLGN3 improved the phosphorylation level of Akt and upregulated the transcription activity of the FOXO family hence promoting tumor proliferation (30). In addition, HOMER3, a member of HOMER (Homer protein) together with WBP2 plays a significant role in glioma invasion (31). For instance, in leukemia, HOMER3 inhibits expression of Bcl2 thus influencing the cell cycle (32). Activity-regulated cytoskeleton (ARC) associated protein causes the internalization of AMAPR from the postsynaptic membrane hence regulating the synapse strength. Through CaM kinase II modulatin, ARC promotes the neurite development in neuroblastoma (33, 34). As a multidomain scaffolding protein, CASK interacts with several cytoplasmic adaptor proteins including Mint1, Reelin, and NR2b by modulating synapse development and synaptic function (35-37). Previous studies demonstrated that CASK is upregulated in various tumors including, colorectal tumor, esophageal cancer (38, 39).

Through Cox regression analysis in univariate and multivariate models, four hub SAPs were screened out, including GRIK2, GABRD, GRID2, and ARC. TCGA cohort served as the training set, and a risk model was constructed to predict the prognosis of LGG patients based on the hub SAPs. The ROC curve analysis confirmed that the risk model exhibited a better diagnostic capacity in identifying LGG patients with poor prognosis. Besides, a nomogram and calibration plots were built to predict 3, and 5 years OS. Using the Kaplan-Meier method, we evaluated the prediction capability of the model in the CGGA cohort, whose results was consistent with that in the TCGA cohort. GRIK2 and GRID2, belonging to inotropic glutamatergic receptors were shown to participate in neurodegeneration and psychiatric diseases, such

as autism, Huntington disease, and major depression (40, 41). There have been a few reports describing the relationship between these genes and cancers. A study by Zhang *et al.* demonstrated that the expression of GABRD might be negatively correlated with infiltrated macrophage in LGGs (42). However, a better understanding of the molecular mechanisms of these four SAPs in glioma is paramount.

Several studies have discovered that seizure is the most prevalent symptom in glioma. Anti-epileptic drugs play a significant role in the combined treatment of glioma (43, 44). Glioma and glutamate disrupt the cortical networks and evoke peritumoral epileptic conditions (45, 46). Neuron-glioma synapse plays the “bidirectional switch” role. On the one hand, AMAP-induced current promotes post-synaptic glioma proliferation, and in turn, glioma increases neuronal activity through NGS, causing neuronal hyperexcitability and seizures (13, 47, 48). Interestingly, our findings attested that GABRD were upregulated in the glioma tissue of patients with glioma-associated epilepsy compared to those in non-epileptic patients,

Conclusion

In this study, we explored the prognostic value and expression of synapse associated proteins LGG. Results revealed that the differentially expressed SAPs potentially participate in the formation of glutamate synapse, and synapse in LGG. We constructed the prognostic model of four SAPs genes signature which acted as an independent prognostic factor in LGG. For the first time, our findings demonstrated that SAPs influence the pathogenesis of LGG, glioma-associated seizure, and can potentially be novel prognostic molecular markers in glioma.

Abbreviations

SAP: synapse associated protein

TCGA: The Cancer Genome Atlas

CGGA: Chinese Glioma Genome Atlas

GEO: gene expression omnibus

LGG: lower-grade glioma

DEG: differentially expressed gene

Declarations

Ethics approval and informed consent

The study was approved by the Research Ethics Committee of Guangdong Provincial People’s hospital, Guangdong Academy of Medical Science (No. GDREC20190145H(R2)). All patients provided written

informed consent.

Consent for publication

Not applicable

Availability of data and material

The datasets analyzed during the current study are available in the gene expression omnibus database (GEO, http://www.ncbi.nlm.nih.gov/geo), The Cancer Genome Atlas database (TCGA, https://portal.gdc.cancer.gov/) and Chinese Glioma Genome Atlas (CGGA, http://www.cgga.org.cn/).

Competing interests

The authors declare that they have no competing interests.

Authors' contributions

HL and CXH designed the study, checked the data, and prepared the manuscript. YY and JTZ performed data collection and statistical analysis. GZL and RM searched the literature and took part in the manuscript preparation. PHX, SWC and YJZ conduct the experiment. PW and DZ supervised this project. All authors read and approved the final manuscript.

Funding

This program was financially supported by Natural Science Foundation of China (NO.81901250), High-level Hospital Construction Project of Guangdong Province of China (NO.DFJH201924) and Natural Science Foundation of Guangdong Province of China (NO.2018A0303130236).

Acknowledgements

We would like to thank Mr. Zongtai Zheng, Mr. Zesen Chen, Mr. Edison Zhang for the data processing and people who contribute to public biomedical databases.

References

1. Louis DN, Perry A, Reifenberger G, von Deimling A, Figarella-Branger D, Cavenee WK, et al. The 2016 World Health Organization Classification of Tumors of the Central Nervous System: a summary. Acta Neuropathol. 2016;131(6):803-20.
2. Ostrom QT, Gittleman H, Truitt G, Boscia A, Kruchko C, Barnholtz-Sloan JS. CBTRUS Statistical Report: Primary Brain and Other Central Nervous System Tumors Diagnosed in the United States in 2011-2015. Neuro Oncol. 2018;20(suppl_4):iv1-iv86.
3. Delev D, Heiland DH, Franco P, Reinacher P, Mader I, Staszewski O, et al. Surgical management of lower-grade glioma in the spotlight of the 2016 WHO classification system. J Neurooncol.

2019;141(1):223-33.
4. Leitch B. Ultrastructure of electrical synapses: review. Electron Microsc Rev. 1992;5(2):311-39.
5. Torrealba F, Carrasco MA. A review on electron microscopy and neurotransmitter systems. Brain Res Brain Res Rev. 2004;47(1-3):5-17.
6. Lane-Donovan C, Herz J. ApoE, ApoE Receptors, and the Synapse in Alzheimer's Disease. Trends Endocrinol Metab. 2017;28(4):273-84.
7. Cao M, Wu Y, Ashrafi G, McCartney AJ, Wheeler H, Bushong EA, et al. Parkinson Sac Domain Mutation in Synaptojanin 1 Impairs Clathrin Uncoating at Synapses and Triggers Dystrophic Changes in Dopaminergic Axons. Neuron. 2017;93(4):882-96.e5.
8. Bhattacharya MR, Geisler S, Pittman SK, Doan RA, Weihl CC, Milbrandt J, et al. TMEM184b Promotes Axon Degeneration and Neuromuscular Junction Maintenance. J Neurosci. 2016;36(17):4681-9.
9. Kattimani Y, Veerappa AM. Dysregulation of NRXN1 by mutant MIR8485 leads to calcium overload in pre-synapses inducing neurodegeneration in Multiple sclerosis. Mult Scler Relat Disord. 2018;22:153-6.
10. Pak C, Danko T, Zhang Y, Aoto J, Anderson G, Maxeiner S, et al. Human Neuropsychiatric Disease Modeling using Conditional Deletion Reveals Synaptic Transmission Defects Caused by Heterozygous Mutations in NRXN1. Cell Stem Cell. 2015;17(3):316-28.
11. Plowey ED, Johnson JW, Steer E, Zhu W, Eisenberg DA, Valentino NM, et al. Mutant LRRK2 enhances glutamatergic synapse activity and evokes excitotoxic dendrite degeneration. Biochim Biophys Acta. 2014;1842(9):1596-603.
12. Zeng Q, Michael IP, Zhang P, Saghafinia S, Knott G, Jiao W, et al. Synaptic proximity enables NMDAR signalling to promote brain metastasis. Nature. 2019;573(7775):526-31.
13. Venkataramani V, Tanev DI, Strahle C, Studier-Fischer A, Fankhauser L, Kessler T, et al. Glutamatergic synaptic input to glioma cells drives brain tumour progression. Nature. 2019;573(7775):532-8.
14. Venkatesh HS, Morishita W, Geraghty AC, Silverbush D, Gillespie SM, Arzt M, et al. Electrical and synaptic integration of glioma into neural circuits. Nature. 2019;573(7775):539-45.
15. Venkatesh HS, Tam LT, Woo PJ, Lennon J, Nagaraja S, Gillespie SM, et al. Targeting neuronal activity-regulated neuroligin-3 dependency in high-grade glioma. Nature. 2017;549(7673):533-7.
16. Shen K. Molecular mechanisms of target specificity during synapse formation. Curr Opin Neurobiol. 2004;14(1):83-8.
17. Colón-Ramos DA. Synapse formation in developing neural circuits. Curr Top Dev Biol. 2009;87:53-79.
18. Jüttner R, Rathjen FG. Molecular analysis of axonal target specificity and synapse formation. Cell Mol Life Sci. 2005;62(23):2811-27.
19. Cerami E, Gao J, Dogrusoz U, Gross BE, Sumer SO, Aksoy BA, et al. The cBio Cancer Genomics Portal: An Open Platform for Exploring Multidimensional Cancer Genomics Data. Cancer Discovery. 2012;2(5):401-4.

20. Gao J, Aksoy BA, Dogrusoz U, Dresdner G, Gross B, Sumer SO, et al. Integrative analysis of complex cancer genomics and clinical profiles using the cBioPortal. Sci Signal. 2013;6(269):pl1.
21. Kuol N, Stojanovska L, Apostolopoulos V, Nurgali K. Role of the nervous system in cancer metastasis. J Exp Clin Cancer Res. 2018;37(1):5.
22. Palm D, Entschladen F. Neoneurogenesis and the neuro-neoplastic synapse. Prog Exp Tumor Res. 2007;39:91-8.
23. Herner A, Sauliunaite D, Michalski CW, Erkan M, De Oliveira T, Abiatari I, et al. Glutamate increases pancreatic cancer cell invasion and migration via AMPA receptor activation and Kras-MAPK signaling. Int J Cancer. 2011;129(10):2349-59.
24. Magnon C, Hall SJ, Lin J, Xue X, Gerber L, Freedland SJ, et al. Autonomic nerve development contributes to prostate cancer progression. Science. 2013;341(6142):1236361.
25. Ni T, Huang T, Gu SL, Wang J, Liu Y, Sun X, et al. DRG Neurons Promote Perineural Invasion of Endometrial Cancer via GluR2. J Cancer. 2020;11(9):2518-28.
26. Venkataramani V, Tanev DI, Strahle C, Studier-Fischer A, Fankhauser L, Kessler T, et al. Glutamatergic synaptic input to glioma cells drives brain tumour progression. Nature. 2019;573(7775):532-8.
27. Venkatesh HS, Morishita W, Geraghty AC, Silverbush D, Gillespie SM, Arzt M, et al. Electrical and synaptic integration of glioma into neural circuits. Nature. 2019;573(7775):539-45.
28. Yool AJ, Ramesh S. Molecular Targets for Combined Therapeutic Strategies to Limit Glioblastoma Cell Migration and Invasion. Front Pharmacol. 2020;11:358.
29. Liu R, Qin XP, Zhuang Y, Zhang Y, Liao HB, Tang JC, et al. Glioblastoma recurrence correlates with NLGN3 levels. Cancer Med. 2018;7(7):2848-59.
30. Li Z, Gao W, Fei Y, Gao P, Xie Q, Xie J, et al. NLGN3 promotes neuroblastoma cell proliferation and growth through activating PI3K/AKT pathway. Eur J Pharmacol. 2019;857:172423.
31. Chen S, Zhang Y, Wang H, Zeng YY, Li Z, Li ML, et al. WW domain-binding protein 2 acts as an oncogene by modulating the activity of the glycolytic enzyme ENO1 in glioma. Cell Death Dis. 2018;9(3):347.
32. Li Z, Qiu HY, Jiao Y, Cen JN, Fu CM, Hu SY, et al. Growth and differentiation effects of Homer3 on a leukemia cell line. Asian Pac J Cancer Prev. 2013;14(4):2525-8.
33. Donai H, Sugiura H, Ara D, Yoshimura Y, Yamagata K, Yamauchi T. Interaction of Arc with CaM kinase II and stimulation of neurite extension by Arc in neuroblastoma cells expressing CaM kinase II. Neurosci Res. 2003;47(4):399-408.
34. DaSilva LL, Wall MJ, L PdA, Wauters SC, Januário YC, Müller J, et al. Activity-Regulated Cytoskeleton-Associated Protein Controls AMPAR Endocytosis through a Direct Interaction with Clathrin-Adaptor Protein 2. eNeuro. 2016;3(3).
35. Porter AP, White GRM, Mack NA, Malliri A. The interaction between CASK and the tumour suppressor Dlg1 regulates mitotic spindle orientation in mammalian epithelia. J Cell Sci. 2019;132(14).

36. Stafford RL, Ear J, Knight MJ, Bowie JU. The molecular basis of the Caskin1 and Mint1 interaction with CASK. J Mol Biol. 2011;412(1):3-13.
37. Huang TN, Hsueh YP. CASK point mutation regulates protein-protein interactions and NR2b promoter activity. Biochemical and biophysical research communications. 2009;382(1):219-22.
38. Wei JL, Fu ZX, Fang M, Zhou QY, Zhao QN, Guo JB, et al. High expression of CASK correlates with progression and poor prognosis of colorectal cancer. Tumour Biol. 2014;35(9):9185-94.
39. Wang Q, Lu J, Yang C, Wang X, Cheng L, Hu G, et al. CASK and its target gene Reelin were co-upregulated in human esophageal carcinoma. Cancer Lett. 2002;179(1):71-7.
40. Kalkan Z, Durasi İ M, Sezerman U, Atasever-Arslan B. Potential of GRID2 receptor gene for preventing TNF-induced neurodegeneration in autism. Neurosci Lett. 2016;620:62-9.
41. Zeng W, Gillis T, Hakky M, Djoussé L, Myers RH, MacDonald ME, et al. Genetic analysis of the GRIK2 modifier effect in Huntington's disease. BMC Neurosci. 2006;7:62.
42. Zhang H, Zhang L, Tang Y, Wang C, Chen Y, Shu J, et al. Systemic screening identifies GABRD, a subunit gene of GABAA receptor as a prognostic marker in adult IDH wild-type diffuse low-grade glioma. Biomed Pharmacother. 2019;118:109215.
43. van Breemen MS, Rijsman RM, Taphoorn MJ, Walchenbach R, Zwinkels H, Vecht CJ. Efficacy of anti-epileptic drugs in patients with gliomas and seizures. J Neurol. 2009;256(9):1519-26.
44. Goldstein ED, Feyissa AM. Brain tumor related-epilepsy. Neurol Neurochir Pol. 2018;52(4):436-47.
45. Campbell SL, Buckingham SC, Sontheimer H. Human glioma cells induce hyperexcitability in cortical networks. Epilepsia. 2012;53(8):1360-70.
46. Rudà R, Trevisan E, Soffietti R. Epilepsy and brain tumors. Curr Opin Oncol. 2010;22(6):611-20.
47. Labrakakis C, Patt S, Hartmann J, Kettenmann H. Glutamate receptor activation can trigger electrical activity in human glioma cells. Eur J Neurosci. 1998;10(6):2153-62.
48. Osswald M, Jung E, Sahm F, Solecki G, Venkataramani V, Blaes J, et al. Brain tumour cells interconnect to a functional and resistant network. Nature. 2015;528(7580):93-8.

Tables

Table 1: The primer of hub SAPs

Gene	Forward	Reverse
ARC	5’-GTTCATCGTTCTGCCTTGTC-3’	5’-CAGCCTTGAGGATTGGTTATG-3’
GRID2	5’-GCAACAGGAATGATGACTACAC T -3’	5’-CAGGCATACTCTGTGACCACT-3’
GRIK2	5’- TGATGTTGAGCCCTACCGATA-3’	5’-GTTCCATCGACCACTTTTCAATG-3’
GABRD	5’-AGAGCTACGGTTACTCATCGG-3’	5’- GGCCAGCGGACTTGAAGTT -3’
GAPDH	5’-GCCATCACAGCAACACAGAA-3’	5’- GCCATACCAGTAAGCTTGCC -3’

Table 2: differentially expressed synapse associated proteins (SAPs) in lower-grade gliomas

Category	genes	number
Upregulated synapse associated proteins	LRFN4, DHX36, CASK, EGLN1, PTN, FCGR2B, NTRK2, EIF4EBP1, ABHD17C, TTYH1, GRIA4, SSH1, IL1RAP, SRGN, ARC, CHRNA1, DBN1, SYT6, ACTL8, GRIK4, CEL, CACNG4, ARF4, CACNG6, ITSN1, FBXO45, ZNF804A, CAPRIN1, NLGN4X, LRP4, KPTN, SLC7A11, PTPRS, GRIK3, PDLIM5, NEDD4, PFN1, HOMER3, CACNG7, SEMA3F, CTTNBP2, LRRC4B, FYN, GHRL, NLGN2, POTEKP, GRIA3, NLGN1, EIF4A3, CRIPT, GRIK2, MAGI2, NLGN3, PLCB3, CYFIP1, HCLS1, ZMYND8, TANC2, DAG1, APOE, EPHB2, GRIK5, NLGN4Y, NRP2, FGF22, CRKL, CDH2, GRID2	68
Downregulated synapse associated proteins	PIN1, SYT5, STX1B, NGEF, HOMER1, GABRA1, NEFL, SYNPR, CACNB3, LZTS3, GABRA5, SRCIN1, SYN1, PPFIA2, DLG2, NRXN3, GRIN2B, GRIN2A, GABRA2, SV2A, CACNA1E, WASF1, SNAP91, NEFH, CACNA1B, CDK5, CDK5R1, EPHA4, NRN1, LRFN2, GRM5, CALB1, SYP, INA, SYN2, CACNG3, GABRB1, SNAP25, CAMKV, GABRD, PRKCG, CAMK2B, NCS1, ITPKA	44

Figures

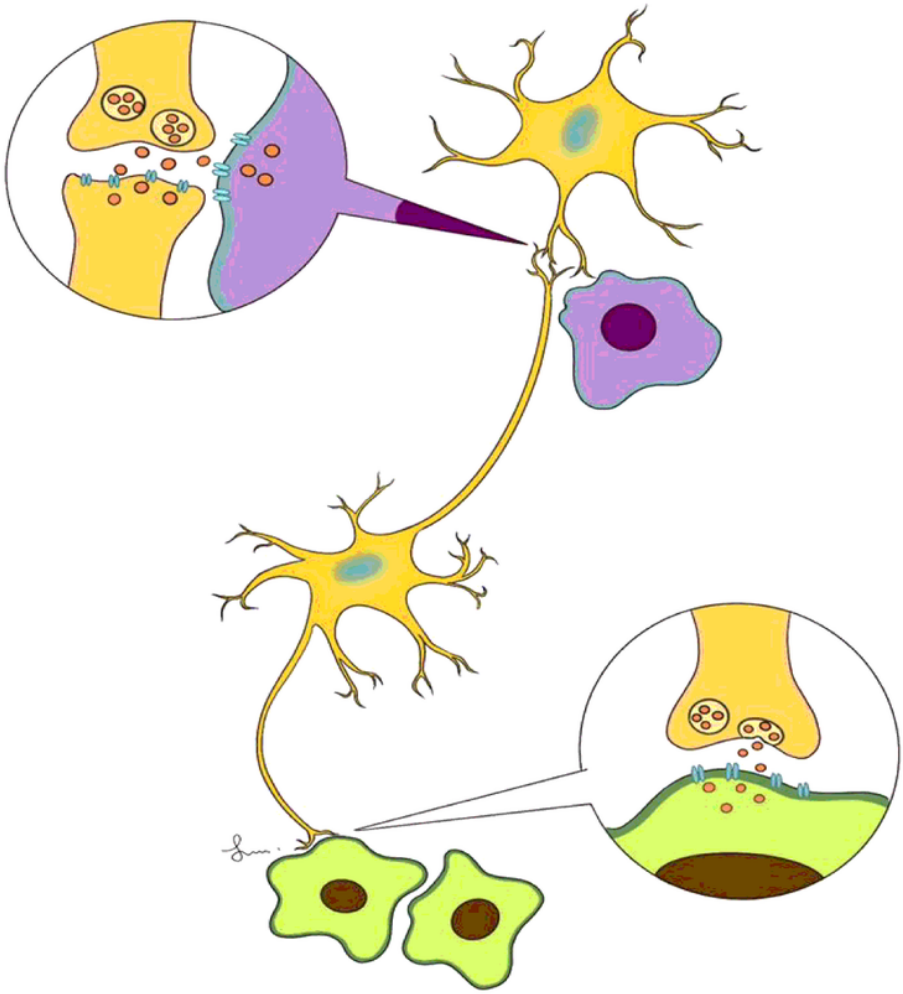

Figure 1

Represents a model of a neuron-tumor synapse. Yellow cells represent neurons; Purple cell represent the breast brain metastasis; the green cell represent the glioma cells. The tumor cells form a synapse like structure with neurons.

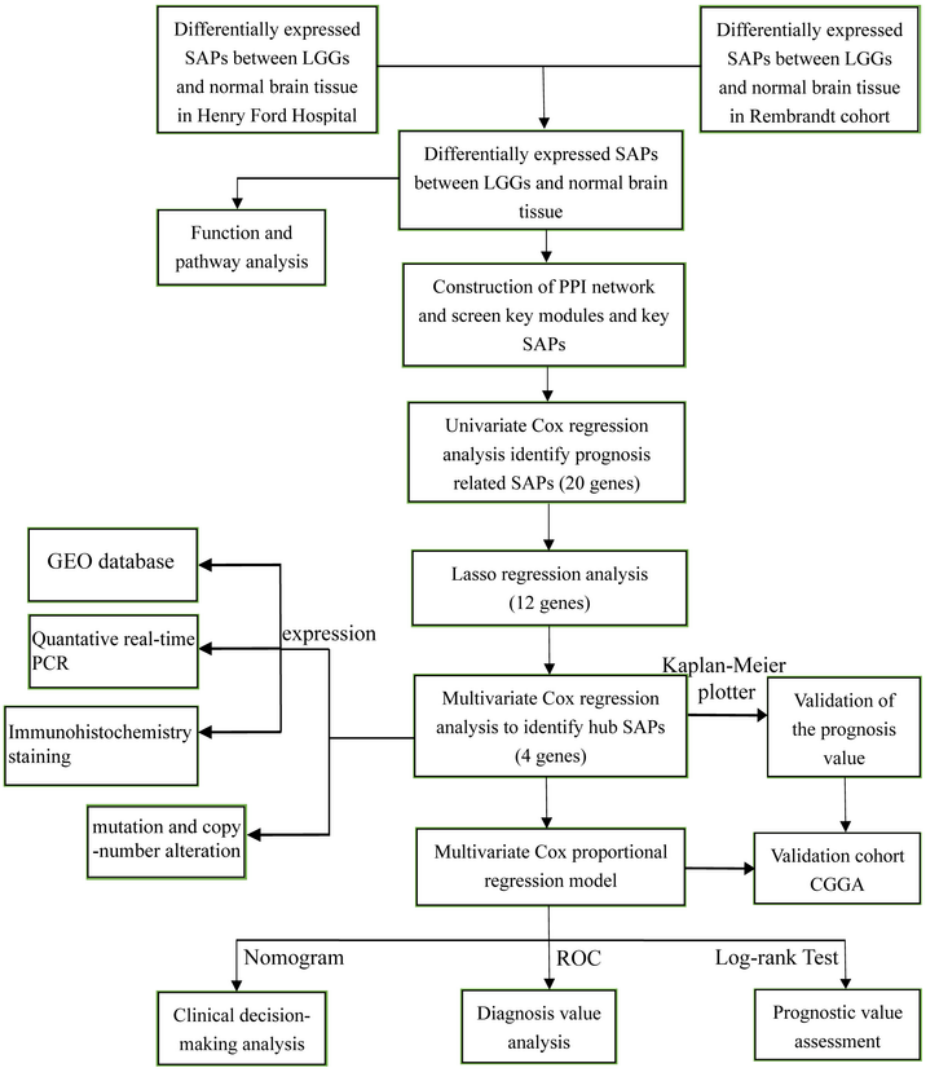

Figure 2

Whole procedures for analyzing synapse associated protein (SAPs) in lower-grade glioma (LGG).

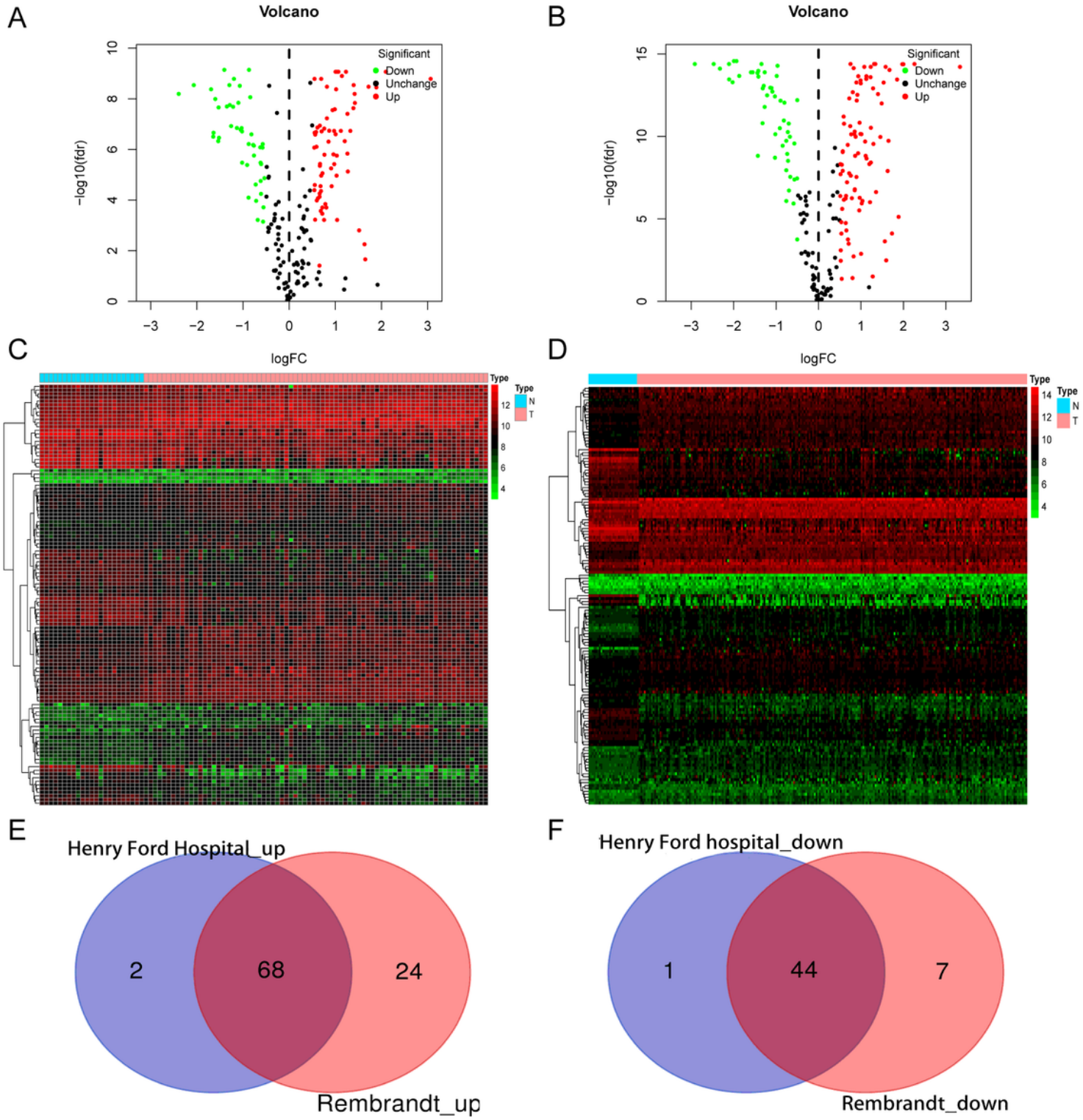

Figure 3

Volcano plot and heatmap showing the differentially expressed SAPs between LGG and normal brain tissues in the Rembrandt cohort and Henry Ford cohort, respectively (A-D). Venn showing common upregulated SAPs and downregulated SAPs in both cohorts (E, F).

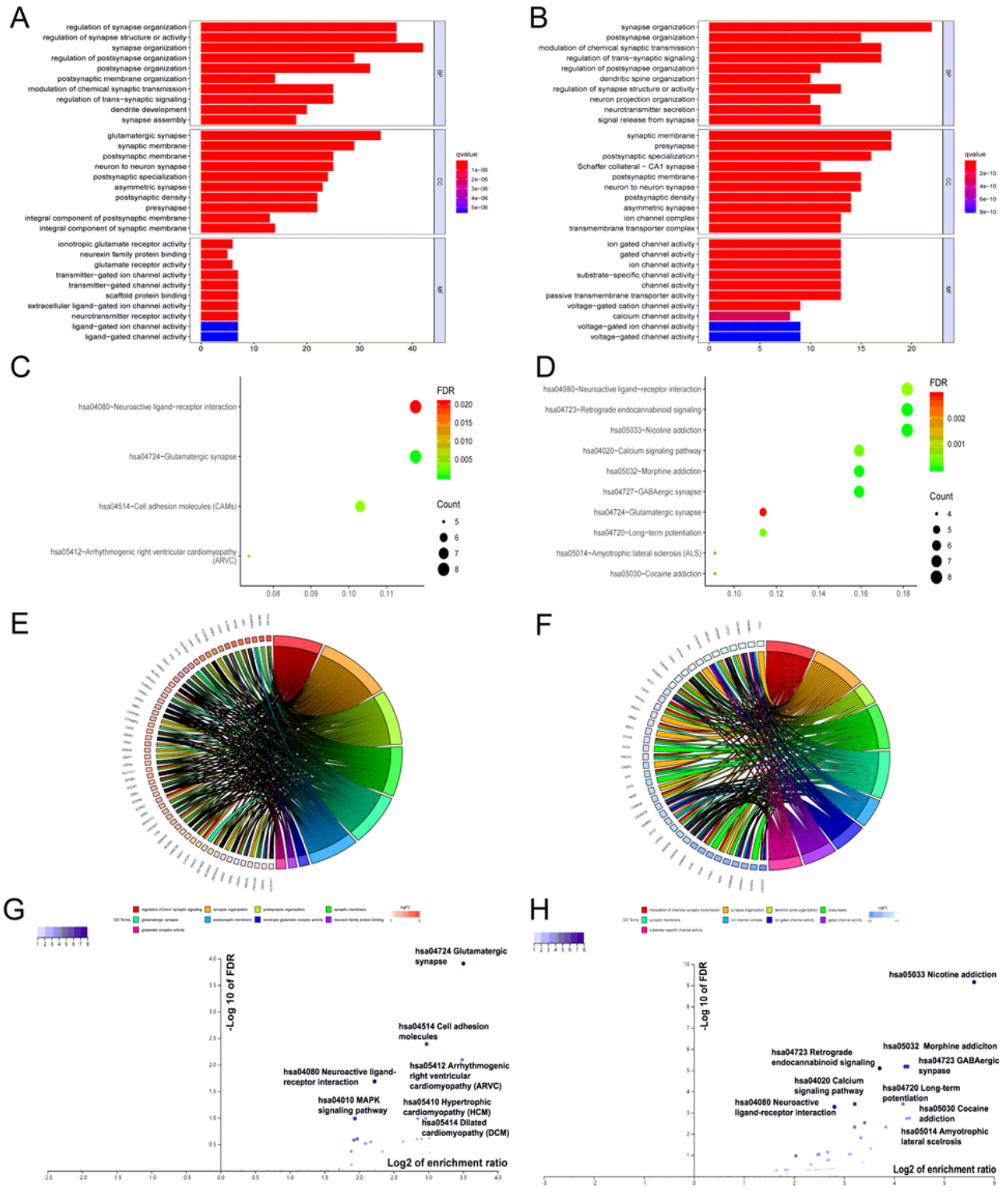

Figure 4

Function enrichment analysis on differentially expressed SAPs. Bar plots respectively show the GO term upregulated SAPs or downregulated SAPs enriched in (A, B). A bubble plot showing results of KEGG analyses for the upregulated SAPs (C) and downregulated SAPs (D). WEB-based Gene Set Analysis Toolkit was used to validate the result of GO analysis (E and F) and KEGG (G and H).

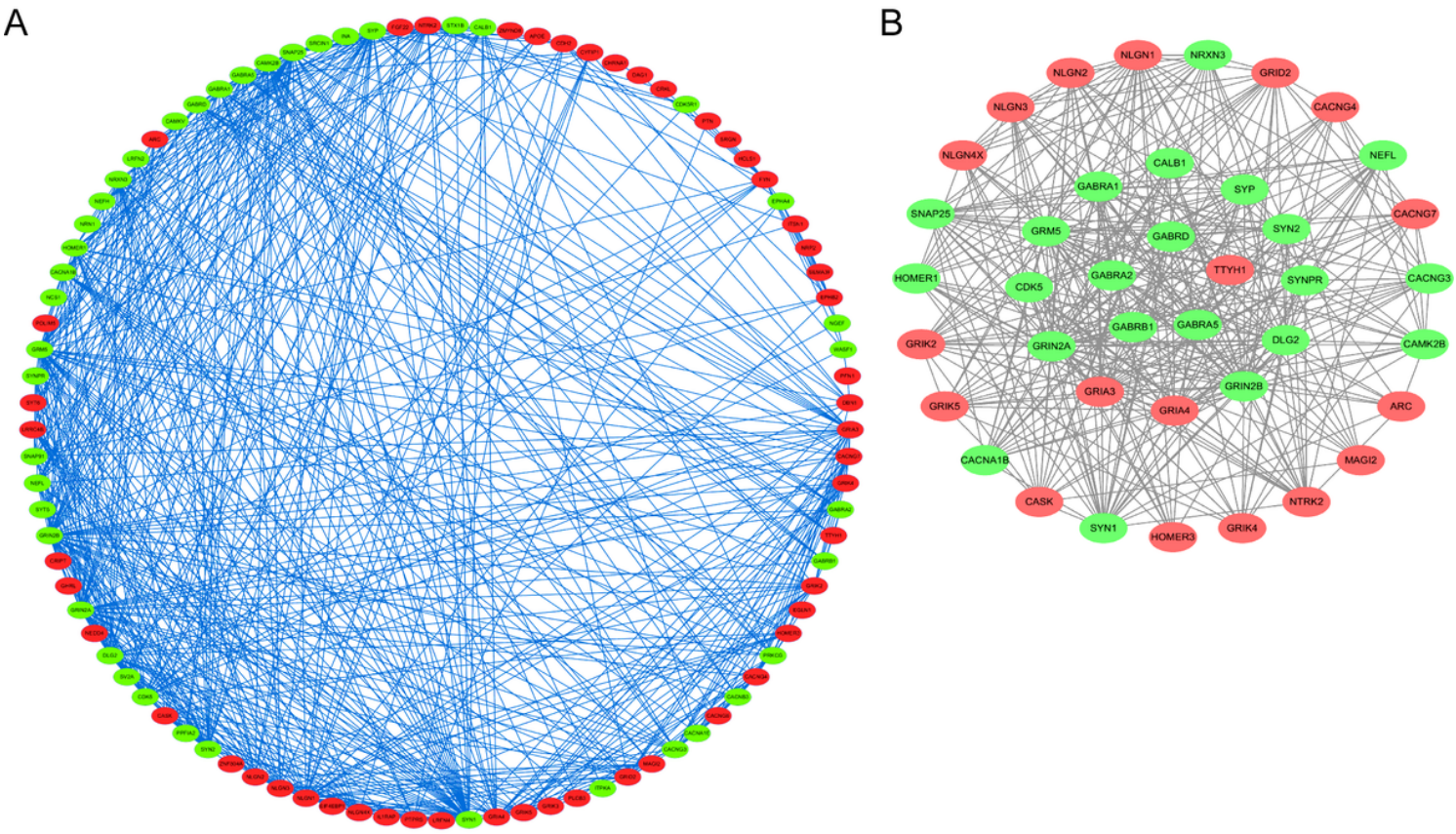

Figure 5

Protein-protein interaction network and module associated with SAPs. (A) Protein-protein interaction network of differentially expressed SAPs, (B) key modules from the PPI network. Green circles: down-regulation; red circles: upregulation.

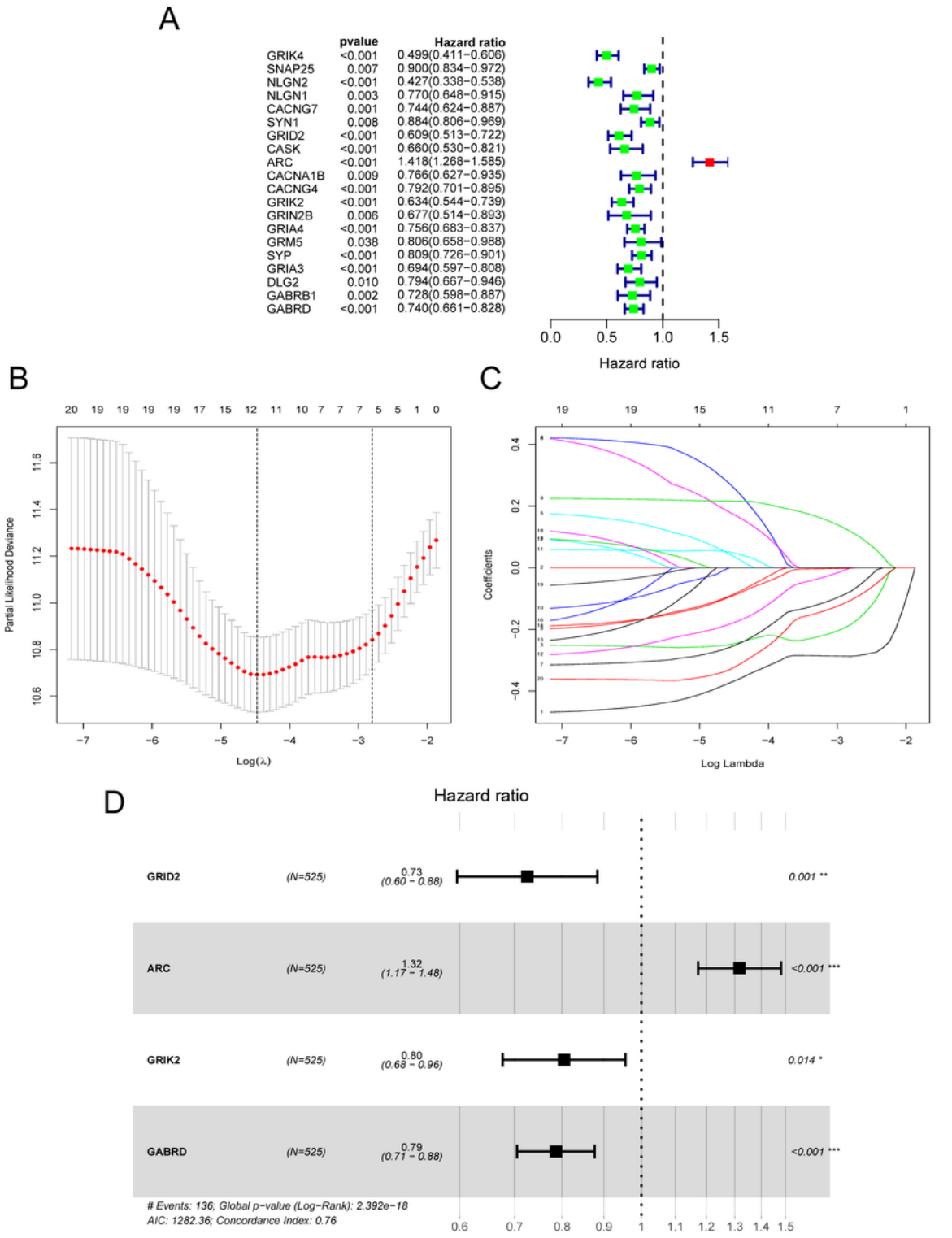

Figure 6

Identification of hub SAPs. Univariate Cox regression analysis performed to identify hub SAPs in the training dataset (A). Lasso regression analysis of key SAPs in the training dataset (B and C). Multivariate Cox regression analysis of key SAPs (D). *, P<0.05; **, P<0.01; ***, P<0.001.

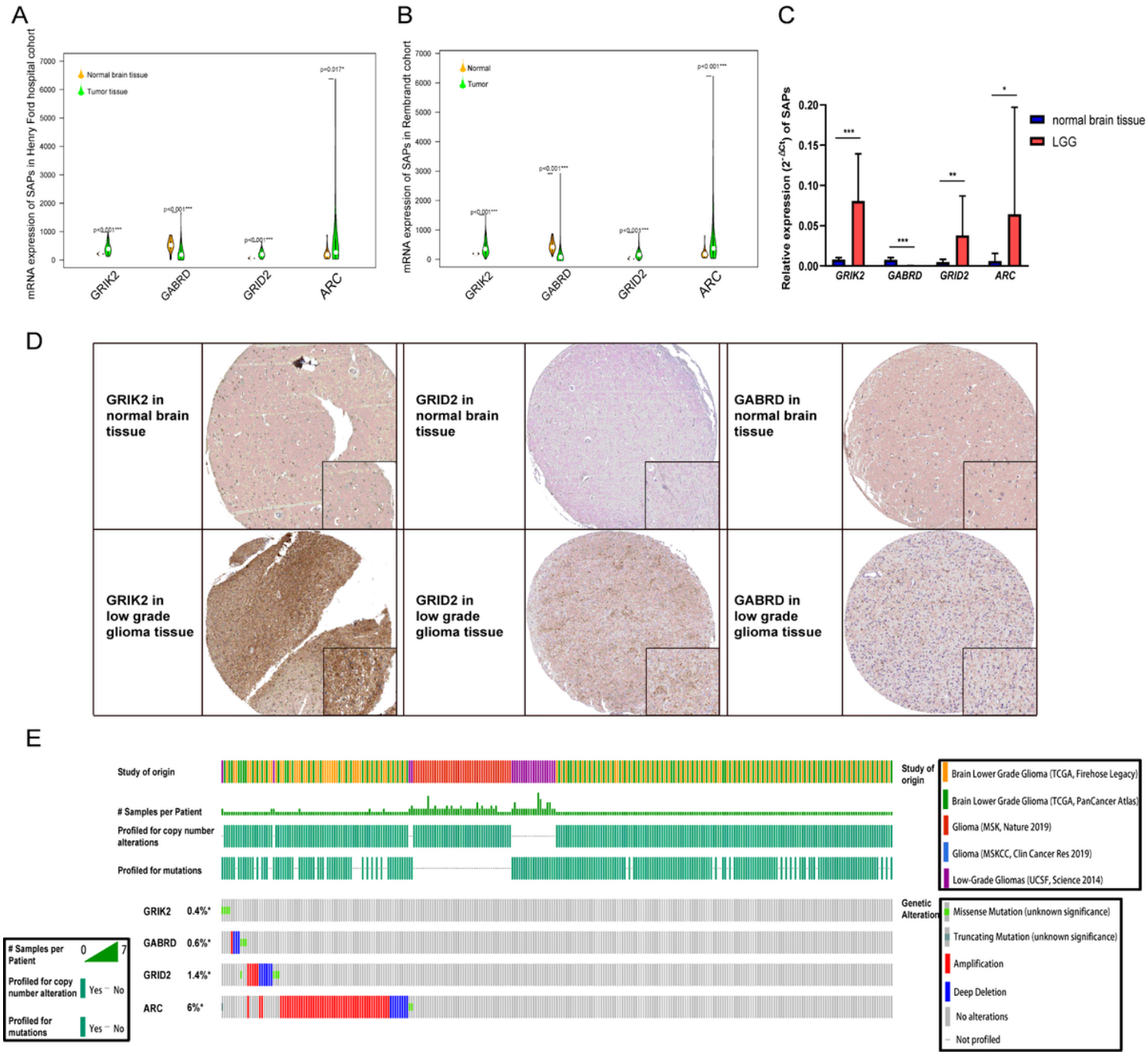

Figure 7

Hub SAPs expression and alteration analysis in LGGs. Gene expression of hub SAPs between LGGs and normal brain tissue (A, B); Validation of protein expression of hub genes in normal brain tissue and LGGs by means of the quantitative real-time PCR (C) and HPA database (D); Genetic alteration of each hub gene (E). *, P<0.05; **, P<0.01; ***, P<0.001.

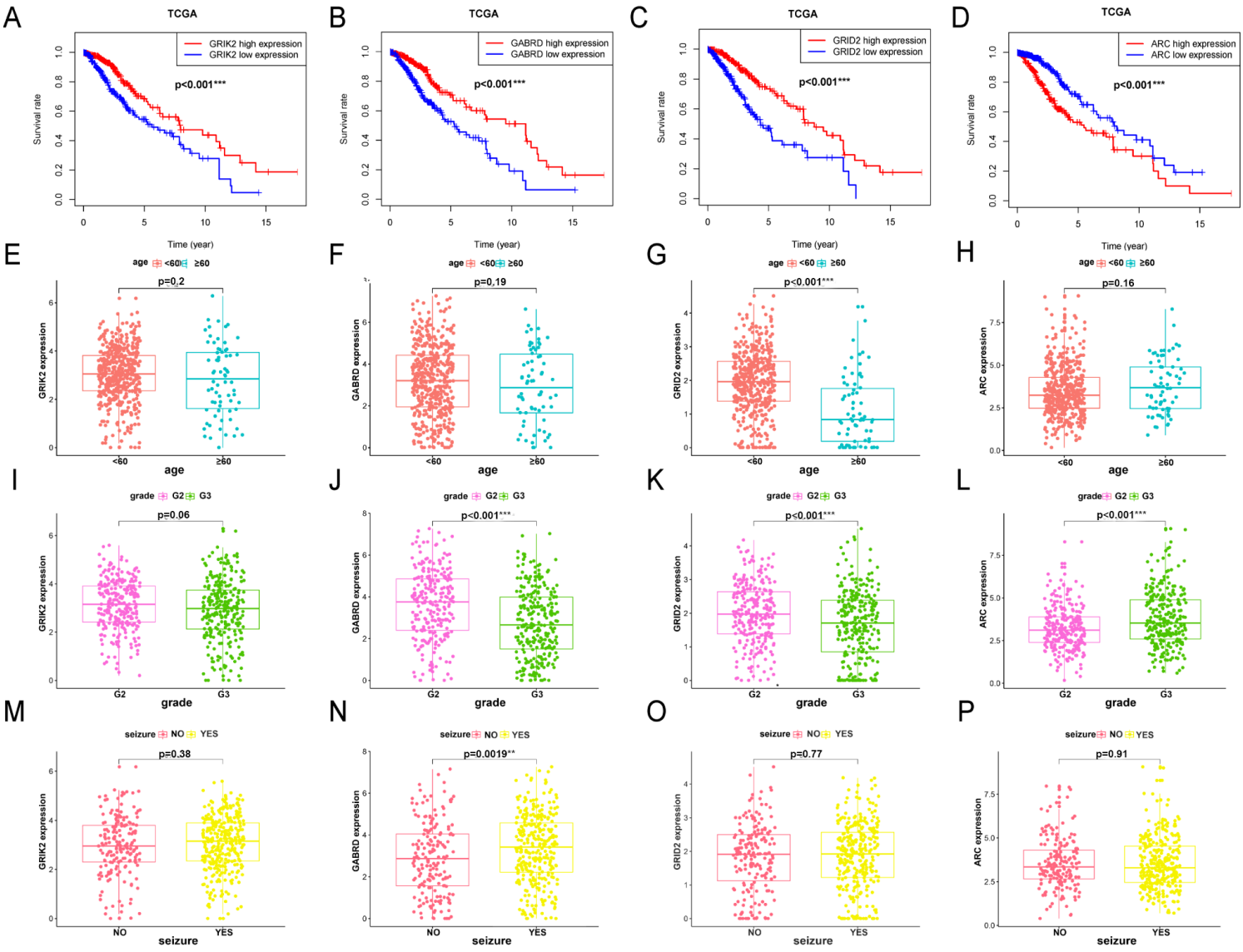

Figure 8

Prognostic value and clinical characteristics of hub four SAPs in LGGs. The prognostic value of GRIK2 (A); GABRD (B); GRID2 (C); ARC (D). The expression characteristics of hub SAPs in different age (E-H), grade (I-L), seizure or not (M-P). *, P<0.05; **, P<0.01; ***, P<0.001.

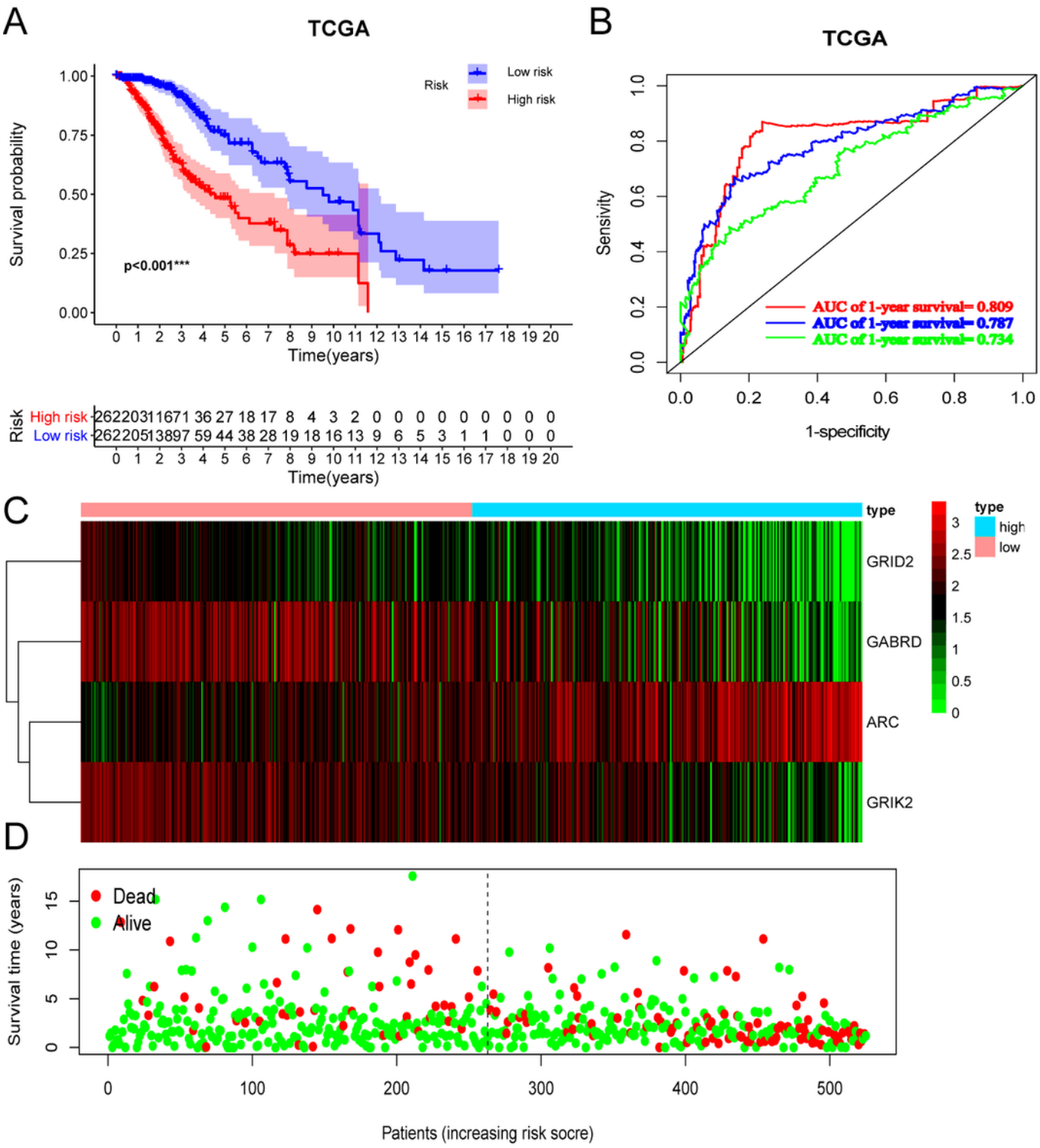

Figure 9

Risk score analysis of the four-SAPs signature model in TCGA. Survival analysis according to risk score in LGG of TCGA cohort (A); ROC analysis on TCGA cohort (B); the heatmap show the difference of hub SAP between low-risk group and high-risk group (C); survival status of patients in TCGA cohort (D). *, P<0.05; **, P<0.01; ***, P<0.001.

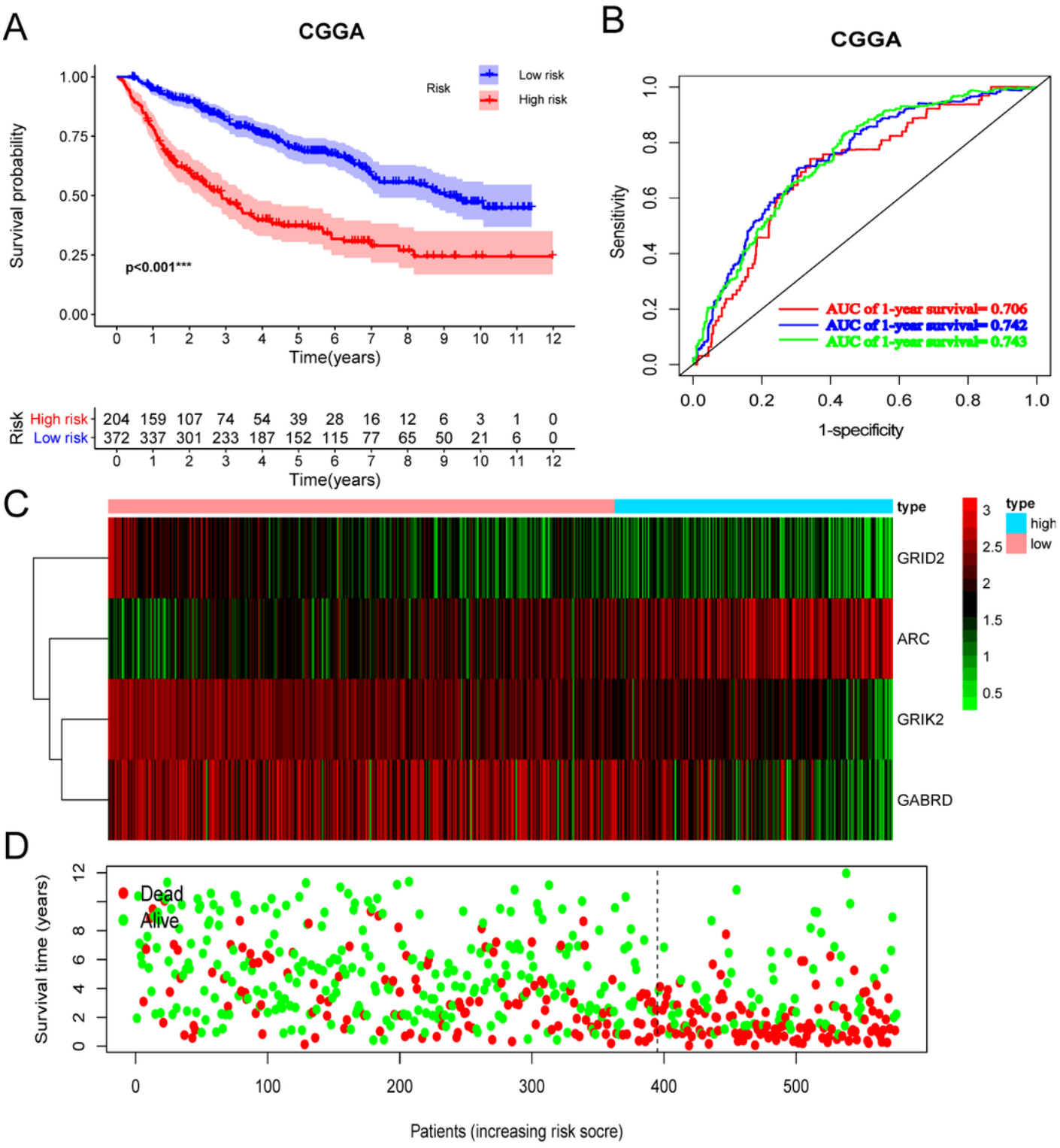

Figure 10

Survival analysis according to risk score in LGG of CGGA cohort (A); ROC analysis on CGGA cohort (B); the heatmap show the difference of hub SAP between low-risk group and high-risk group (C); survival status of patients in the CGGA cohort (D). *, P<0.05; **, P<0.01; ***, P<0.001.

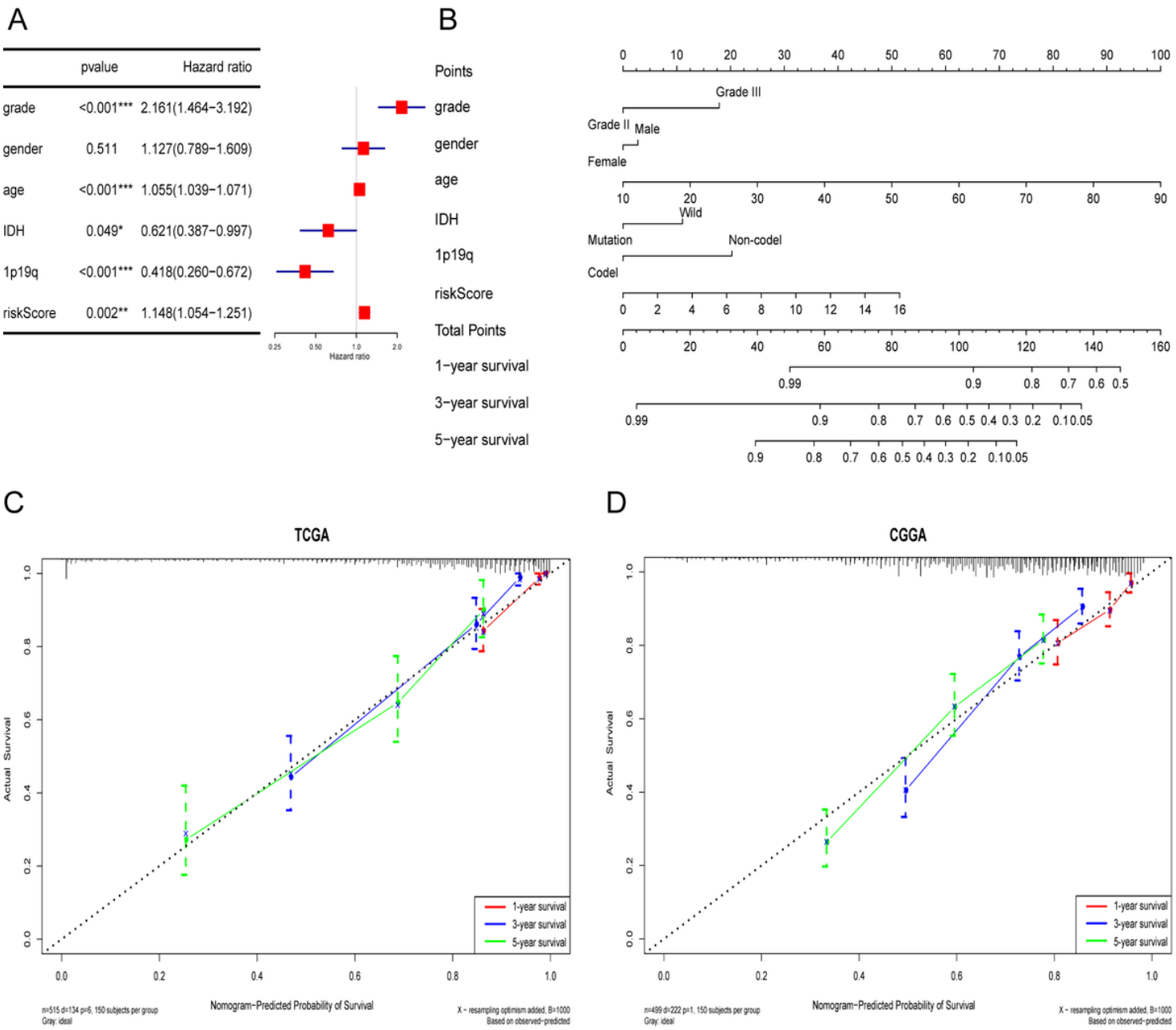

Figure 11

Nomogram and calibration plots of risk-signature and clinicopathologic factors. Multivariate Cox regression analysis showed the risk score was an independent prognostic factor in LGGs (A). Nomogram to predict 1-, 3- and 5-year OS in the TCGA cohort (B). Calibration plots of the nomogram to predict OS at 1, 3, and 5 years in the TCGA and CGGA cohorts (C and D). *, P<0.05; **, P<0.01; ***, P<0.001.

Supplementary Files

This is a list of supplementary files associated with this preprint. Click to download.

- supplementaryfig1.tif

- SupplementTable1.xlsx